

Electrocardiogram signal analysis for R-peak detection and denoising with hybrid linearization and principal component analysis

Harjeet KAUR*, Rajni RAJNI

Department of Electrical and Computer Engineering, Faculty of Electronics and Communication Engineering,
Shaheed Bhagat Singh State Technical Campus, Ferozepur, Punjab, India

Received: 09.04.2016

Accepted/Published Online: 18.08.2016

Final Version: 29.05.2017

Abstract: In the areas of biomedical and healthcare, electrocardiogram (ECG) signal analysis is one of the major aspects of research. The accuracy in the detection of subtle characteristic features in ECG is of great significance. This paper deals with an algorithm based on hybrid linearization and principal component analysis for ECG signal denoising and R-peak detection. The ECG data have been taken from the MIT-BIH Arrhythmia Database for performance evaluation. The signal is denoised by applying the hybrid linearization method, which is an arrangement of the extended Kalman filter along with discrete wavelet transform, and then principal component analysis is employed to detect R waves and the QRS complex. The reported work has been implemented in the MATLAB environment for 25 different ECG records yielding 99.90% sensitivity, 99.97% positive predictivity, and a detection error rate of 0.120%. The achieved performance outperforms the recent research done in the area of interest.

Key words: Electrocardiogram, denoising, extended Kalman filter, wavelet decomposition, principal component analysis

1. Introduction

The contraction and relaxation of the cardiac muscles in the heart drives blood throughout the body and occurs throughout the lifespan of a person [1]. The systole and diastole of the cardiovascular muscle tissues are coordinated by an association of nerve cells to a wavelike activity. This may be imaged with echocardiography, which uses the heart imaging principle. Another reliable noninvasive diagnostic tool that monitors the electrical activity of the heart is electrocardiography. In electrocardiography, the recorded graphical trace is known as an electrocardiogram (ECG), which corresponds to the magnitude and direction of the electrical activity of the heart. The long-term recording of an ECG provides an effectual way for the detection of cardiac diseases [2,3]. Additionally, it can reveal the identity of a person [4]. One cardiac cycle consists of three major constituent waves: the P component wave, QRS complex, and T component wave [5]. The QRS complex is the most significant event in the ECG waveform [6]. A typical ECG wave with these components is shown in Figure 1 [7].

In the ECG signal, clinically significant information is found in the amplitude of different peaks and intervals of constituent waves. Consequently, the development of procedures for quick and precise ECG denoising and QRS complex detection, and particularly for the R-peak, is required for automatic ECG analysis [8]. Several attempts have been reported in the literature, including adaptive Kalman filters [9] and adaptive wavelets with Wiener filtering [10]. Due to the nonstationary characteristics of ECG signals and the noise present in them,

*Correspondence: sandhu.harjit75@gmail.com

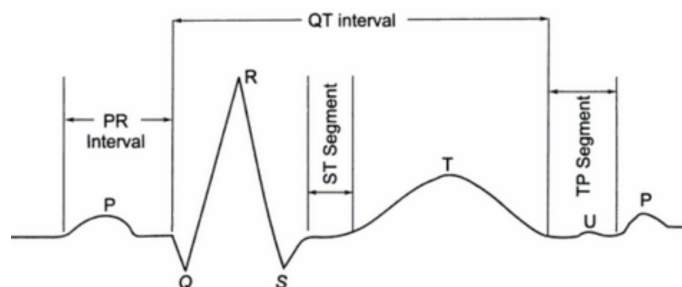


Figure 1. A typical ECG waveform [7].

Wiener filters cannot provide good results [11]. Pan and Tompkins implemented a real-time algorithm in assembly language to detect the QRS complex [12]. This QRS detector failed to detect 0.675% of beats. Studies revealed that ECG features can be extracted using empirical mode decomposition (EMD), discrete wavelet transform (DWT), and adaptive thresholding with wavelet bases in [13–15], respectively. Other methods for QRS complex detection include the zero crossing detector [16] and Hilbert transform [17]. Researchers have also applied a singularity method on EMD filtered ECG signals for detection of the QRS complex [18]. In [19], a model based on finding locations, widths, and magnitudes from ECG waves was proposed to extract features. A wavelet ECG detector based on a combination of a multiscaled product algorithm with a soft-thresholding function for effective detection of the QRS complex was demonstrated in [20]. For QRS complex detection, the use of the Hilbert transform with an adaptive threshold was explored in [8]. However, investigators applied band pass filtering on ECG signals before applying the Hilbert transform since it does not improve the signal-to-noise ratio [8].

Over the past several years, a number of ECG denoising and beat detection methods have been reported by researchers. In spite of this, a universally accepted solution has not been found yet. The presented work focuses on principal component analysis (PCA) along with thresholding for the detection of the QRS complex and the R-peak. The concept of PCA involves projection of data along the direction of the highest variance [21]. As it is complex to investigate and extract accurate features from ECG signals due to the presence of noise, a hybrid linearization method (HLM) involving two influential tools, the extended Kalman filter (EKF) with discrete wavelet transform (DWT), is presented for denoising. Thereafter, PCA is applied to noise-free ECG signals for extraction of the R-peak and QRS complex. The novelty of the proposed work is the approach of adopting three different prevailing tools, i.e. EKF, DWT, and PCA, for denoising, detection of constituent components and important peaks of the ECG signal, and achieving superior results in comparison to other techniques.

This paper is organized in five sections. After the introduction of the topic of interest and work done in the relevant field in Section 1, materials and methods for the current approach are summarized in Section 2. Section 3 explores the methodology for the current work and Section 4 provides results and a discussion. Finally, the paper is concluded in Section 5.

2. Materials and methods

2.1. Arrhythmia Database and Matrix Laboratory (MATLAB)

The MIT-BIH arrhythmia database has been utilized for the evaluation of the proposed work [22]. The database consists of 48 half-hour ECG recordings with a sampling frequency of 360 Hz. The ECG signals from this database include irregular heart rhythms, wider and low amplitude QRS complex, paced rhythms,

ventricular tachycardia, atrial and ventricular flutter, atrial and ventricular fibrillation, premature ventricular contraction, sinus bradycardia including baseline wanders, and muscle artifacts [23]. The presented work has been implemented with MATLAB software. The MATLAB environment provides a simpler platform with various built-in functions and a toolbox that leads to a convenient way for ECG signal processing with great accuracy [24].

2.2. Extended Kalman filter

The conventional Kalman filters are applicable for linear models only, but in practice most of the applications and realistic systems of interest are nonlinear in nature [25]. For extending the functionality of the Kalman filter to nonlinear dynamic structures, a modified variant of it, the EKF, has been developed [26,27]. For a discrete, nonlinear system $x_{k+1} = f(x_k, w_k)$ and its observation $y_k = g(x_k, v_k)$, linear approximation close to a reference point $(\hat{x}_k, \hat{w}_k, \hat{v}_k)$ can be formulated [28] as in Eq. (1):

$$\begin{cases} x_{k+1} \approx f(\hat{x}_k, \hat{w}_k) + A_k(x_k - \hat{x}_k) + F_k(w_k - \hat{w}_k) \\ y_k \approx g(\hat{x}_k, \hat{v}_k) + C_k(x_k - \hat{x}_k) + G_k(v_k - \hat{v}_k) \end{cases} \quad (1)$$

where x_k and y_k are the state and observation vectors, respectively. The function $f(\cdot)$ represents state evolution and $g(\cdot)$ defines the relation between observations and state. The parameters v_k and w_k represent measurement and state noise with $R_k = E\{v_k v_k^T\}$ and $Q_k = E\{w_k w_k^T\}$ covariance matrices, respectively. A_k , C_k , F_k and G_k are the Jacobian matrices as shown in Eq. (2):

$$\begin{cases} A_k = \left. \frac{\partial f(x, \hat{w}_k)}{\partial x} \right|_{x_k = \hat{x}_k} & F_k = \left. \frac{\partial f(\hat{x}_k, w_k)}{\partial w} \right|_{w = \hat{w}_k} \\ C_k = \left. \frac{\partial g(x, \hat{v}_k)}{\partial x} \right|_{x = \hat{x}_k} & G_k = \left. \frac{\partial g(\hat{x}_k, v)}{\partial v} \right|_{v = \hat{v}_k} \end{cases} \quad (2)$$

Hence, for implementing the EKF algorithm, the measurement and time propagation equations are expressed below in Eqs. (3) and (4), respectively:

$$\begin{cases} \hat{x}_{k/k-1} = f(\hat{x}_{k-1/k-1}, 0) \\ P_{k/k-1} = A_k P_{k-1/k-1} A_k^T + F_k Q_k F_k^T \end{cases} \quad (3)$$

$$\begin{cases} \hat{x}_{k/k} = \hat{x}_{k/k-1} + K_k [y_k - g(\hat{x}_{k/k-1}, 0)] \\ K_k = P_{k/k-1} C_k^T [C_k P_{k/k-1} C_k^T + G_k^T]^{-1} \\ P_{k/k} = P_{k/k-1} - K_k C_k P_{k/k-1} \end{cases} \quad (4)$$

where $\hat{x}_{k/k-1} = E x_k | y_{k-1}, y_{k-2}, \dots, y_1$ is the estimate of the state vector at instant k using y_1 to y_{k-1} observations. $\hat{x}_{k/k} = E x_k | y_k, y_{k-1}, \dots, y_1$ is the estimate of the state vector at instant k using y_1 to y_k observations and K_k is the filter gain. $P_{k/k-1}$ and $P_{k/k}$ are described in a similar manner. The EKF facilitates linearization and denoising of ECG signals [29].

2.3. Wavelet transform

Wavelet transform (WT) is a powerful tool to study nonstationary signals like ECGs. The WT provides a description of a signal in the time–frequency domain [30,31] and works on a multiscale basis [32]. WT is

appropriate for all frequencies since it has a variable size window, i.e. being narrow in high frequency ranges and broad in low frequency ranges [33]. The WT of signal $y(t)$ is expressed [15] as in Eq. (5):

$$W_a y(b) = \frac{1}{\sqrt{a}} \int_{-\infty}^{\infty} y(t) \psi\left(\frac{t-b}{a}\right) dt \tag{5}$$

where a is the dilation parameter, b is the translation parameter, and $\psi(t)$ is the wavelet function.

WT is categorized into DWTs and continuous wavelet transforms (CWTs).

2.4. Discrete wavelet transform

In recent years, DWT has been established as a convincing tool in signal processing as it provides good frequency resolution at low frequencies and good time resolution at high frequencies. The two-level wavelet decomposition of a signal $y(n)$ is depicted in Figure 2. The low-pass $h(n)$ and high-pass $g(n)$ filters are used during decomposition of the input signal. At the first level, decomposition results in detail (D1) and approximation (A1) coefficients as the ECG signal is passed through the arrangement of complementary filters. The process continues as the coefficient A1 is further decomposed at the second level using the same procedure.

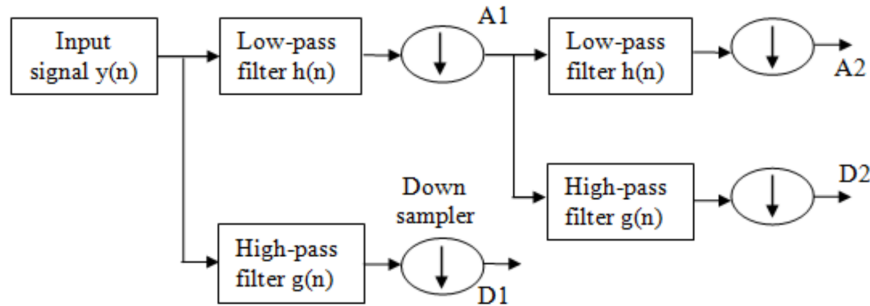


Figure 2. Two-level wavelet decomposition.

2.5. Hybrid linearization method

The EKF makes the ECG signal noise-free to some extent. The HLM, which involves application of the EKF in combination with the DWT, is implemented to improve the quality of ECG signals available at the EKF output [29]. The Bior3.1 wavelet is preferred over other wavelet functions due to its lower mean square error (MSE) and higher signal-to-noise ratio (SNR) values [34]. Additionally, it provides lower percentage root mean square difference and higher peak SNR values. The performance of the hybrid linearization (HL) algorithm is evaluated by two parameters, SNR (in dB) and MSE, as described in Eqs. (6) and (7), respectively [28]:

$$SNR [dB] = \left(\frac{\sum_i |x(i)|^2}{\sum_i |x(i) - \hat{x}(i)|^2} \right) \tag{6}$$

$$MSE = \frac{\sum_i (x(i) - \hat{x}(i))^2}{N} \tag{7}$$

where $x(t)$ is the actual ECG signal, $\hat{x}(t)$ is the smooth reconstructed version of the signal, and N is the number of samples.

2.6. Principal component analysis

PCA is a linear dimensionality reduction technique [21]. It is a statistical method interested in delineating the covariance configuration of data sets. The PCA technique includes the calculation and decomposition of a covariance matrix (obtained from data) into eigenvectors and eigenvalues [21,23]. The eigenvectors are organized in descending order of eigenvalues and finally the data are projected in the directions of sorted eigenvectors [23,35]. The general steps involved in PCA are described below [8]:

1. Calculation of the mean of the original ECG signal x_i from Eq. (8):

$$\bar{x} = \frac{1}{M} \sum_{i=1}^M x_i \quad (8)$$

where x_i is represented by an $M \times N$ data matrix and \bar{x} is the mean of signal. M and N are the number of samples of a beat and observations of beats, respectively.

2. Subtraction of the mean from the original ECG signal as shown in Eq. (9):

$$xadj = x_i - \bar{x} \quad (9)$$

3. Calculation of the covariance matrix from the data as in Eq. (10). The measurement of covariance between a dimension and itself will give the variance of that dimension.

$$C = \frac{1}{M-1} \sum_{i=1}^M (x_i - \bar{x})^T (x_i - \bar{x}) \quad (10)$$

4. Computation of the eigenvectors e_i and the diagonal matrix of eigenvalues λ_i as calculated below in Eq. (11):

$$C e_i = \lambda_i e_i, \quad i = 1, \dots, N \quad (11)$$

5. Formation of a feature vector by selecting components. The eigenvectors are arranged in descending order of their eigenvalues and dimensions are reduced by selecting the K components. In practice, K is selected to retain the physiological information so that the performance is acceptable in clinical aspects [36]. For each eigenvalue, the percentage of variation r_K is achieved by applying Eq. (12):

$$r_K = \frac{\sum_{i=1}^K \lambda_i}{\sum_{i=1}^N \lambda_i} \quad (12)$$

Furthermore, we may select the components with percentage of variation more than the threshold percentage (th), which is 0.95 or 0.9 [8], as expressed in Eq. (13):

$$\hat{r}_K = (r_K \geq th) \quad (13)$$

6. Finally, a new data set is derived as shown in Eq. (14):

$$\text{New data set} = (\hat{r}_K)^T (xadj)^T \quad (14)$$

3. Proposed methodology

The ECG signal is processed for denoising and detection of the R-peak and QRS complex. The different stages involved in processing are explained as follows:

1. The preprocessing stage includes acquisition of real ECG records into the MATLAB environment from the MIT-BIH Arrhythmia Database (mitdb) [22].
2. The next step in the ECG processing is denoising, i.e. elimination of baseline wander and high frequency noise. For this, the HL algorithm is implemented to remove noises.
3. After preprocessing, the noise-free ECG signal is decomposed using PCA. During detection, eigenvalues are squared for minimizing smaller values and maximizing larger values. Then thresholding is done to retain R-peaks (larger eigenvalues).
4. With reference to the detected R-peaks, Q and S peaks are extracted. The denoised signal is scanned for 50 ms on the left as well as on the right of the R-peak to obtain the minimum value. The minimum values on the left and right correspond to the Q-peak and S-peak, respectively, hence forming a complete QRS complex.

The performance of the detection algorithm is evaluated in terms of sensitivity (Se), positive predictivity (P+), and detection error rate (DER), which are described in Eqs. (15), (16), and (17), respectively:

$$Se = \frac{\text{True positive}}{\text{True positive} + \text{False negative}} \times 100\% \quad (15)$$

$$P+ = \frac{\text{True positive}}{\text{True positive} + \text{False positive}} \times 100\% \quad (16)$$

$$DER = \frac{\text{False positive} + \text{False negative}}{\text{True positive}} \times 100\% \quad (17)$$

where the true positive (TP) rate is correctly detected R-peaks, false negative (FN) is undetected R-peaks, and false positive (FP) refers to misdetections. The different phases involved in the proposed algorithm for ECG signal processing with the HLM and PCA are illustrated in Figure 3.

4. Results and discussion

The ECG analysis begins with the preprocessing stage. The extraction of accurate cardiologic information from the signal becomes difficult due to the presence of various noises [37]. In an ECG signal, muscle artifacts occur due to electrode skin impedance and baseline drift is caused by patient movement, breathing, or coughing. The morphological characteristics of an ECG wave may vary drastically due to artifacts and severe baseline wandering. These undesirable noise contaminants are required to be removed prior to any additional signal processing to provide an accurate signal analysis. Difficulties also arise during detection of the QRS complex due to the low SNR of ECG signals, i.e. noisy signals. Therefore, the proposed approach has been applied to exploit the potentials of both the EKF and DWT to extract noise-free signals from noisy ECG indices. The HL algorithm is applied to the ECG signal to remove low frequency baseline wander and high frequency artifacts. In the HLM, the ECG signal is first filtered with the EKF. It denoises the ECG to some extent. Furthermore,

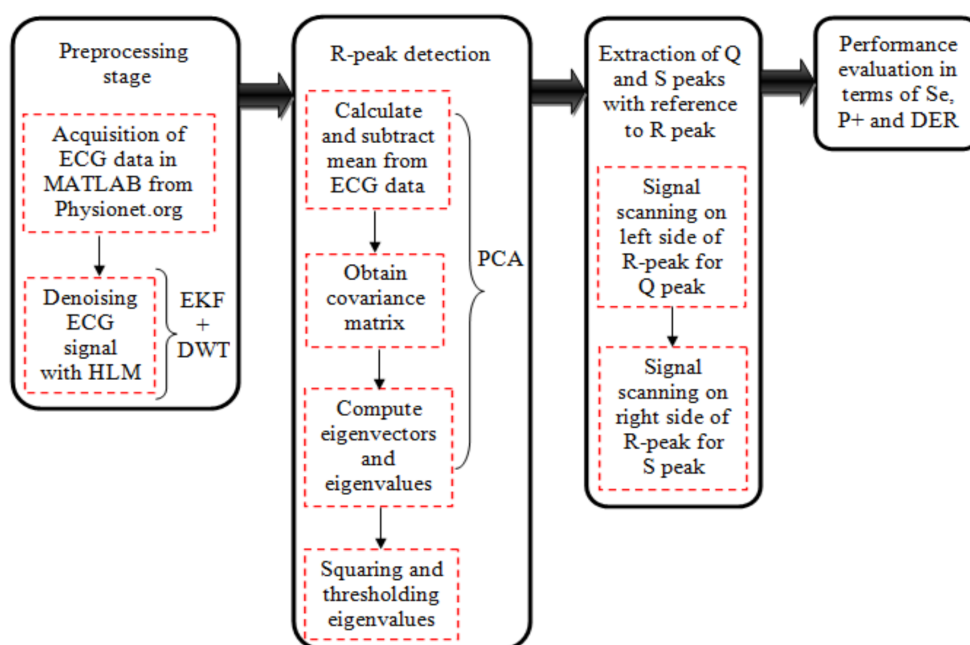


Figure 3. Flow of general stages in proposed methodology.

WT is applied to the filtered signal to enhance the signal quality. During wavelet decomposition, detail and approximation coefficients are extracted and global thresholding is used. The performance of the denoising technique is computed in terms of two important measures, i.e. SNR (in dB) and MSE. The original noisy ECG signal of record mitdb/103 is depicted in Figure 4a and its denoised waveform with removed low and high frequency noises is shown in Figure 4b.

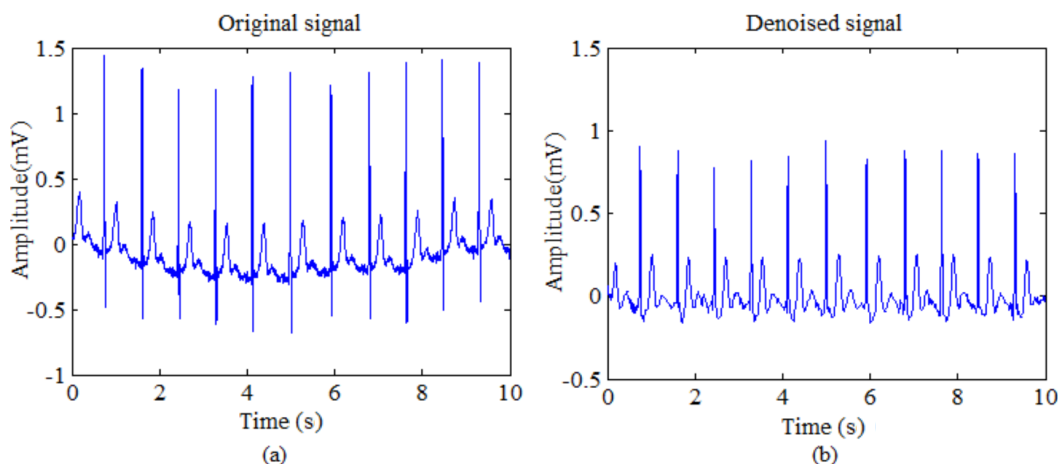


Figure 4. (a) Original ECG signal (record mitdb/103), (b) denoised ECG signal with hybrid linearization method.

From Figure 4a, it is clearly apparent that the signal undergoes a considerable drift and distortion due to the presence of noise, whereas Figure 4b shows an improved ECG signal waveform free from drift after applying the HLM. Although the ECG sample is of 30 min in duration, for simplification it is shown for only 10 s. In Table 1, results of EKF, WT, and HLM filtering are tabulated for comparative study. From the results obtained and depicted in Table 1, it is evident that the SNR has been sufficiently improved with the HL algorithm.

Table 1. Performance evaluation of denoising algorithm.

ECG record cm	EKF		DWT		HLM	
	SNR (dB)	MSE	SNR (dB)	MSE	SNR (dB)	MSE
100	3.8286	5.1e-03	6.9326	2.0e-03	17.4590	1.15e-04
101	3.5305	3.28e-04	3.7445	3.12e-04	11.7044	2.53e-05
103	4.1280	1.04e-02	8.4883	6.0e-03	18.1110	3.61e-04
105	7.2344	1.10e-02	9.0482	1.7e-03	19.3932	8.35e-04
106	3.9266	1.1e-03	5.3831	8.01e-04	12.5836	6.15e-05
108	8.9079	1.47e-02	10.7044	9.7e-03	20.6134	8.66e-04
112	3.5660	1.5e-03	6.6893	7.15e-04	15.0421	5.05e-05
113	3.3690	1.3e-03	6.5621	6.30e-04	15.4663	3.68e-05
114	5.7988	2.06e-02	7.5206	1.4e-03	20.0555	5.38e-04
115	4.8433	1.4e-03	7.3859	7.89e-04	17.4115	4.94e-05
116	6.3323	5.03e-02	8.1179	4.4e-03	17.8918	2.25e-04
117	5.2256	1.81e-02	8.7776	8.0e-03	18.3845	5.70e-04
121	5.3583	7.5e-03	9.9772	2.6e-03	18.8628	2.21e-04
122	3.1873	4.0e-03	3.7663	3.5e-03	12.0947	2.65e-04
123	4.3027	1.0e-02	8.9304	3.5e-03	18.0581	2.40e-04
200	4.0723	3.76e-04	5.8450	2.50e-04	14.8123	2.24e-05
202	6.6418	9.0e-03	9.6953	4.4e-03	19.1839	3.77e-04
205	4.2529	6.76e-04	5.6977	4.84e-04	14.3636	3.78e-05
212	8.4667	2.52e-02	9.0827	2.17e-02	18.9557	2.1e-03
213	5.6996	9.02e-02	7.3913	6.11e-02	17.8650	3.8e-03
215	4.4202	1.72e-02	7.5185	8.43e-03	16.5545	6.02e-04
220	3.8261	4.06e-02	6.6269	1.69e-03	17.7738	8.34e-04
223	6.0924	3.29e-02	8.8749	2.7e-03	19.4381	1.15e-04
231	6.2719	8.0e-03	8.5448	4.7e-03	18.9004	3.13e-04
233	6.5279	4.86e-02	8.9212	2.80e-02	18.7656	2.2e-03

In the ECG signal, the R-peak is the most prominent deflection as the maximum information is concentrated in the region around this peak. The precise detection of the R-peak forms the basis for the detection of other components in the signal. Accurate detection of R-peaks is also necessary to compute the R-R interval, the distance between two adjacent R-peaks, which may be used to detect irregularities in the ECG wave, and the average R-R interval is used to calculate the heart rate [5]. The heart rate derived from an ECG signal can be used to detect cardiac abnormalities such as sinus tachycardia and sinus bradycardia [14]. The R wave can be easily detected due to its higher amplitude than other peaks. In the proposed method, the R wave is detected by squaring and thresholding the eigenvalues obtained with PCA. The detected R wave with PCA is shown in Figure 5.

The indexes of R-peaks marked in Figure 5 are stored for detection of the QRS complex. For detecting the QRS complex, minimum values are searched by scanning the noise-free signal on the left (or right) side of the R-peak for Q (or S) peaks. Figure 6a demonstrates the QRS complex detected from the ECG signal with reference to R-peak indexes and its wider view is shown in Figure 6b.

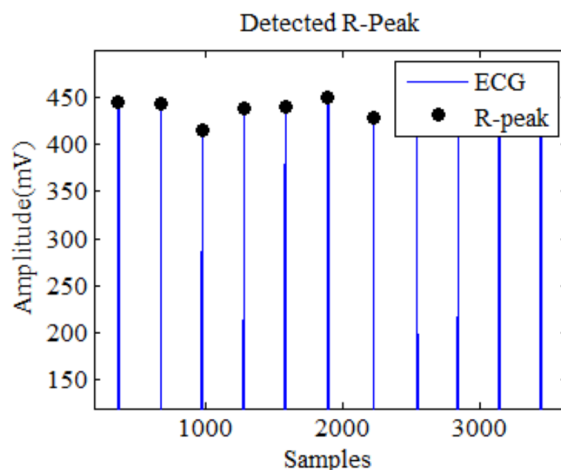


Figure 5. Detected R wave in the ECG signal.

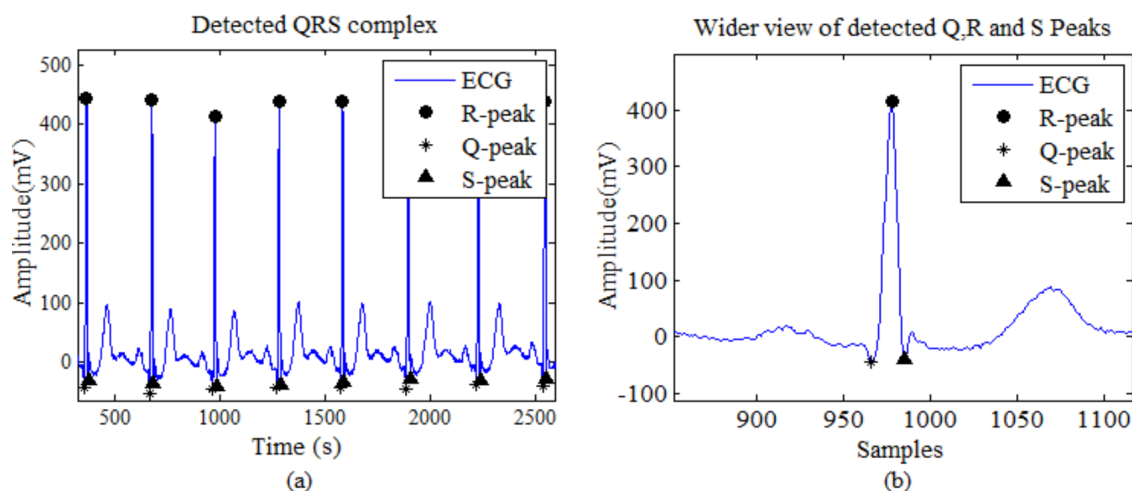


Figure 6. (a) Detected QRS complex of record mitdb/103, (b) wider view of QRS complex.

In Figure 6a, different markers are used to clearly depict the detected Q and S peaks with the R peak, and a wider view of the detected QRS complex is illustrated in Figure 6b for better visibility. From Figures 5, 6a, and 6b, it is notable that the proposed approach successfully detects Q, R, and S peaks. For denoising and detection purposes, different ECG records have been selected from the arrhythmia database with the aim of presenting a comparative performance of the proposed work with recent past studies. The results for the beat detection algorithm are provided in Table 2.

Table 2 depicts the total number of beats, number of detected beats, true positive beats, and false negative and false positive beats. In Table 2, the value of the sensitivity parameter specifies the percentage of heartbeats properly detected by the algorithm and positive predictivity indicates that detected heartbeats are real heartbeats. A comparison of the proposed beat detection algorithm with previous methods is shown in Table 3.

In Table 3, for ECG signals from serial order 1 to 14 and from 15 to 22, the proposed analysis is compared with the work presented in [8] and [38], respectively. In Table 3, NR signifies not reported. In [8], the authors applied Hilbert transform and adaptive thresholding for beat detection and reported an overall 96.28% of Se

Table 2. Performance evaluation of beat detection algorithm.

ECG	Total	Detected	TP	FP	FN	Se	P+	DER
record	beats	beats	beats	beats	beats	(%)	(%)	(%)
100	2273	2265	2265	0	8	99.6	100	0.353
101	1865	1865	1865	0	0	100	100	0
103	2084	2084	2084	0	0	100	100	0
105	2572	2569	2560	9	12	99.5	99.6	0.820
106	2027	2027	2027	0	0	100	100	0
108	1774	1774	1774	0	0	100	100	0
112	2539	2538	2538	0	1	99.9	100	0.039
113	1795	1795	1795	0	0	100	100	0
114	1879	1874	1874	0	5	99.7	100	0.266
115	1953	1953	1953	0	0	100	100	0
116	2412	2410	2410	0	2	99.9	100	0.082
117	1535	1535	1535	0	0	100	100	0
121	1863	1861	1862	1	1	99.9	99.9	0.107
122	2476	2476	2476	0	0	100	100	0
123	1518	1516	1516	0	2	99.8	100	0.131
200	2601	2601	2601	0	0	100	100	0
202	2136	2135	2134	1	2	99.9	99.9	0.140
205	2656	2654	2653	1	3	99.8	99.9	0.150
212	2748	2748	2748	0	0	100	100	0
213	3251	3250	3250	0	1	99.9	100	0.030
215	3363	3362	3359	3	4	99.8	99.9	0.208
220	2048	2048	2048	0	0	100	100	0
223	2605	2604	2604	0	1	99.9	100	0.038
231	1573	1570	1570	0	3	98.8	100	0.191
233	3079	3073	3072	1	7	99.7	99.9	0.260
Total	56625	56587	56573	16	52	99.90	99.97	0.120

and 99.71% of P+. In [38], 99.85% Se, 99.92% P+, and 0.221% DER were reported for R-peak detection with DWT, whereas the proposed beat detection approach measures Se of 99.90%, P+ of 99.97%, and DER of 0.120%. Therefore, it is clearly seen from Tables 2 and 3 that our proposed scheme achieves superior detection rates and outperforms the techniques illustrated in the literature.

5. Conclusion

The detection of ECG signals is closely related to examination and diagnosis of cardiac status. In the presented work, ECG signal analysis is carried out by the method of HLM and PCA. The denoising of ECG wave is a prerequisite to accurate signal processing. In the reported work, ECG signal denoising is achieved successfully through the new approach of HLM, which uses a combination of EKF and DWT to remove baseline wander and muscle artifacts, and hence HLM yields improved SNR and MSE, confirming its superiority over other techniques. Furthermore, the most important part of any ECG signal analysis technique for cardiac health

Table 3. Comparison of proposed work with work reported in [8] and [38].

S. No.	ECG record	Se (%)	P+ (%)	DER (%)	Se (%)	P+ (%)	DER (%)
Proposed work					Rodriguez et al., 2015 [8]		
1	101	100	100	0	99.94	99.51	NR
2	103	100	100	0	99.95	100	NR
3	108	100	100	0	96.13	99.93	NR
4	116	99.9	100	0.082	98.82	99.78	NR
5	117	100	100	0	100	99.93	NR
6	121	99.9	99.9	0.107	99.89	99.94	NR
7	200	100	100	0	99.84	99.80	NR
8	202	99.9	99.9	0.140	99.00	99.95	NR
9	205	99.8	99.9	0.150	99.81	99.47	NR
10	213	99.9	100	0.030	99.90	97.44	NR
11	215	99.8	99.9	0.208	98.58	100	NR
12	223	99.9	100	0.038	98.99	100	NR
13	231	99.8	100	0.191	99.87	99.93	NR
14	233	99.7	99.9	0.260	99.77	99.93	NR
Proposed work					Kaur et al., 2016 [38]		
15	100	99.6	100	0.353	99.6	100	0.397
16	101	100	100	0	99.6	99.7	0.693
17	103	100	100	0	100	99.7	0.239
18	112	99.9	100	0.039	99.9	100	0.039
19	113	100	100	0	99.6	99.9	0.391
20	115	100	100	0	100	99.8	0.153
21	122	100	100	0	100	100	0
22	123	99.8	100	0.191	99.8	100	0.198

assessment is the R-peak and QRS complex detection, which is done using PCA and thresholding. The proposed algorithm is tested and validated using a variety of signals from the standard MIT-BIH Arrhythmia Database. The parameters used to analyze the performance of the beat detection algorithm achieve 99.90% sensitivity, 99.97% positive predictivity, and a detection error rate of 0.120%. The values of SNR and MSE for denoising and of Se, P+, and DER for beat detection acquired by our processed algorithm are comparable with many other techniques in the literature. The improved accuracy in detection rates of the proposed method makes it highly consistent and efficient. In the future, an ECG classifier based on heart rate using some artificial neural network models can be proposed to automate the detection and classification of various cardiovascular abnormalities.

References

- [1] Acharya UR. *Advances in Cardiac Signal Processing*. 1st ed. Berlin, Germany: Springer, 2007.
- [2] Pongpon Sri S, Yu XH. An adaptive filtering approach for electrocardiogram (ECG) signal noise reduction using neural networks. *Neurocomputing* 2013; 117: 206-213.
- [3] Ku CT, Hung KC, Wu TC, Wang HS. Wavelet based ECG data compression system with linear quality control scheme. *IEEE T Bio-Med Eng* 2010; 57: 1399-1409.
- [4] Sufi F, Khalil I. Diagnosis of cardiovascular abnormalities from compressed ECG: a data mining based approach. *IEEE T Inf Technol B* 2011; 15: 33-39.

- [5] Banerjee S, Gupta R, Mitra M. Delineation of ECG characteristic features using multiresolution wavelet analysis method. *Measurement* 2012; 45: 474-487.
- [6] Javadi M, Arani SAAA, Sajedin A, Ebrahimpour R. Classification of ECG arrhythmia by a modular neural network based on mixture of experts and negatively correlated learning. *Biomed Signal Proces* 2013; 8: 289-296.
- [7] Reddy DC. *Biomedical Signal Processing: Principles and Techniques*. 1st ed. New Delhi, India: Tata McGraw-Hill, 2005.
- [8] Rodriguez R, Mexicano A, Bila J, Cervantes S, Ponce R. Feature extraction of electrocardiogram signals by applying adaptive threshold and principal component analysis. *J Appl Res Technol* 2015; 13: 261-269.
- [9] Vullings R, Veries BD, Bergmans JWM. An adaptive Kalman filter for ECG signal enhancement. *IEEE T Bio-Med Eng* 2011; 58: 1094-1103.
- [10] Smital L, Vitek M, Kozumplik J, Provaznik I. Adaptive wavelet Wiener filtering of ECG signals. *IEEE T Bio-Med Eng* 2013; 60: 437-445.
- [11] Wu Y, Rangayyan RM, Zhou Y, Ng SC. Filtering electrocardiographic signals using an unbiased and normalized adaptive noise reduction system. *Med Eng Phys* 2009; 31: 17-26.
- [12] Pan J, Tompkins WJ. A real time QRS complex detection algorithm. *IEEE T Bio-Med Eng* 1985; 32: 230-236.
- [13] Slimane ZEH, Nait-Ali A. QRS complex detection using empirical mode decomposition. *Digit Signal Process* 2010; 20: 1221-1228.
- [14] Lin HY, Liang SY, Ho YL, Lin YH, Ma HP. Discrete wavelet transform based noise removal and feature extraction for ECG signals. *IRBM* 2014; 35: 351-361.
- [15] Madeiro JPV, Cortez PC, Oliveira FI, Siqueira RS. A new approach to QRS segmentation based on wavelet bases and adaptive threshold technique. *Med Eng Phys* 2007; 29: 26-37.
- [16] Kohler BU, Hennig C, Orglmeister R. QRS detection using zero crossing counts. *Progress in Biomedical Research* 2003; 8: 138-145.
- [17] Arzeno N, Deng ZD, Poon CS. Analysis of first derivative based QRS detection algorithms. *IEEE T Bio-Med Eng* 2008; 55: 478-484.
- [18] Xing H, Huang M. A new approach for QRS complex detection algorithm based on empirical mode decomposition. In: 2nd International Conference on Bioinformatics and Biomedical Engineering; 16–18 May 2008, Shanghai, China. New York, NY, USA: IEEE. pp. 693-696.
- [19] Zhu J, He L, Gao Z. Feature extraction from a novel ECG model for arrhythmia diagnosis. *Bio-Med Mater Eng* 2014; 24: 2883-2891.
- [20] Min YJ, Kim HK, Kang YR, Kim GS, Park J, Kim SW. Design of wavelet-based ECG detector for implantable cardiac pacemakers. *IEEE T Biomed Circ S* 2013; 7: 426-436.
- [21] Martis RJ, Acharya UR, Min LC. ECG beat classification using, PCA, LDA, ICA and discrete wavelet transform. *Biomed Signal Proces* 2013; 8: 437-448.
- [22] Goldberger AL, Amaral LAN, Glass L, Hausdroff JM, Ivanov PC, Mark RG, Mietus JE, Moody GB, Peng CK, Stanely EH. PhysioBank, PhysioToolkit and PhysioNet: components of a new research resource for complex physiologic signals. *Circulation* 2000; 101: E215-20.
- [23] Martis RJ, Acharya UR, Lim CM, Suri JS. Characterization of ECG beats from cardiac arrhythmia using discrete cosine transform in PCA framework. *Knowl-Based Syst* 2013; 45: 76-82.
- [24] Islam MK, Haque ANMM, Tangim G, Ahammad T, Khandokar MRH. Study and analysis of ECG signal using MATLAB & LABVIEW as effective tools. *Int J Comput Electr Eng* 2012; 4: 404-408.
- [25] Sameni R, Shamsollahi MB, Jutten C, Clifford GD. A nonlinear Bayesian filtering framework for ECG denoising. *IEEE T Bio-Med Eng* 2007; 54: 2172-2185.
- [26] Sayadi O, Shamsollahi MB. ECG denoising and compression using a modified extended Kalman filter structure. *IEEE T Bio-Med Eng* 2008; 55: 2240-2248.

- [27] Roonizi EK, Sassi R. A signal decomposition model-based Bayesian framework for ECG components separation. *IEEE T Signal Proces* 2016; 64: 665-674.
- [28] Quali MA, Chafaa K, Ghanai M, Lorente LM, Rojas DB. ECG denoising using extended Kalman filter. In: 2013 International Conference on Computer Applications Technology; 20–22 January 2013; Sousse, Tunisia. New York, NY, USA: IEEE. pp. 1-6.
- [29] Lakshmi PS, Raju VL. ECG denoising using hybrid linearization method. *TELKOMNIKA Indonesian Journal of Electrical Engineering* 2015; 15: 504-508.
- [30] Akansu AN, Serdijn WA, Selesnick IW. Emerging applications of wavelets: a review. *Physical Communication* 2010; 3: 1-18.
- [31] Daamounche A, Harmami L, Alajlan N, Melgani F. A wavelet optimization approach for ECG signal classification. *Biomed Signal Proces* 2012; 7: 342-349.
- [32] Khorrami H, Moavenian M. A comparative study of DWT, CWT and DCT transformations in ECG arrhythmias classification. *Expert Syst Appl* 2010; 37: 5751-5757.
- [33] Rai HM, Trivedi A, Shukla S. ECG signal processing for abnormalities detection using multiresolution wavelet transform and artificial neural network classifier. *Measurement* 2013; 46: 3238-3246.
- [34] Kaur I, Rajni, Sikri G. Denoising of ECG signal with different wavelets. *International Journal of Engineering Trends and Technology* 2014; 9: 658-661.
- [35] Martis RJ, Acharya UR, Mandana KM, Ray AK, Chakraborty C. Application of principal component analysis to ECG signals for automated diagnosis of cardiac health. *Expert Syst Appl* 2012; 39: 11792-11800.
- [36] Castells F, Laguna P, Sornmo L, Bollmann A, Riog JM. Principal component analysis in ECG signal processing. *EURASIP J Adv Sig Pr* 2007; 2007: 074580.
- [37] Chawla MPS. Detection of indeterminacies in corrected ECG signals using parameterized multidimensional independent component analysis. *Comput Math Method M* 2009; 10: 85-115.
- [38] Kaur I, Rajni, Marwaha A. ECG signal analysis and arrhythmia detection using wavelet transform. *Journal of the Institution Engineers (India) Series B* 2016; 97: 499.